Neuron, Vol. 24, 751–762, November, 1999, Copyright ©1999 by Cell Press

Age-Dependent Emergence and Progression of a Tauopathy in Transgenic Mice Overexpressing the Shortest Human Tau Isoform

Takeshi Ishihara,* Ming Hong,* Bin Zhang,*
Yasushi Nakagawa,* Michael K. Lee,†
John Q. Trojanowski,* and Virginia M.-Y. Lee*‡
*The Center for Neurodegenerative Disease Research
Department of Pathology and Laboratory Medicine
The University of Pennsylvania School of Medicine
Philadelphia, Pennsylvania 19104
†The Laboratory of Neuropathology
The Johns Hopkins School of Medicine
Baltimore, Maryland 21205

Summary

Filamentous tau aggregates are hallmarks of tauopathies, e.g., frontotemporal dementia with parkinsonism linked to chromosome 17 (FTDP-17) and amyotrophic lateral sclerosis/parkinsonism–dementia complex (ALS/PDC). Since FTDP-17 *tau* gene mutations alter levels/functions of tau, we overexpressed the smallest human tau isoform in the CNS of transgenic (Tg) mice to model tauopathies. These mice acquired age-dependent CNS pathology similar to FTDP-17 and ALS/PDC, including insoluble, hyperphosphorylated tau and argyrophilic intraneuronal inclusions formed by tau-immunoreactive filaments. Inclusions were present in cortical and brainstem neurons but were most abundant in spinal cord neurons, where they were associated with axon degeneration, diminished microtubules (MTs), and reduced axonal transport in ventral roots, as well as spinal cord gliosis and motor weakness. These Tg mice recapitulate key features of tauopathies and provide models for elucidating mechanisms underlying diverse tauopathies, including Alzheimer's disease (AD).

Introduction

Tau is an abundant microtubule- (MT-) associated protein in the CNS that is implicated in the pathogenesis of Alzheimer's disease (AD) and a group of neurodegenerative diseases known as "tauopathies" (Goedert et al., 1997). Prototypical tauopathies are exemplified by frontotemporal dementia with parkinsonism linked to chromosome 17 (FTDP-17), amyotrophic lateral sclerosis/parkinsonism–dementia complex (ALS/PDC), and progressive supranuclear palsy (PSP). Like other tauopathies, FTDP-17, PSP, and ALS/PDC are characterized by numerous intraneuronal inclusions formed by aggregated paired helical filaments (PHFs) and/or straight filaments composed of aberrantly phosphorylated tau proteins (PHF-tau) in widespread regions of the brain and spinal cord (Hirano et al., 1961; Tomonaga, 1977; Kato et al., 1986; Matsumoto et al., 1990; Reed et al., 1998; Spillantini et al., 1998a).

Six alternatively spliced tau isoforms are expressed in the adult human CNS (Goedert et al., 1989; Andreadis et al., 1992) and are localized predominantly in axons (Binder et al., 1985). Tau proteins bind to MTs and stabilize MTs in the polymerized state (Weingarten et al., 1975; Drechsel et al., 1992), but the formation of PHF-tau results in a loss of these important functions (Bramblett et al., 1993; Yoshida and Ihara, 1993). Moreover, unlike normal tau, PHF-tau is insoluble, accumulates in the somatodendritic domain of neurons, and assembles into filaments that aggregate as neurofibrillary tangles (NFTs; Lee et al., 1991; Goedert et al., 1997). In addition to PHF-tau, other cytoskeletal proteins, such as neurofilament (NF) subunits and ubiquitin, are also found in many NFTs (Perry et al., 1985; Schmidt et al., 1990).

The massive degeneration of neurons and extensive gliosis associated with the progressive accumulation of PHF-tau lesions provide circumstantial evidence implicating filamentous tau pathology in the onset/progression of neurodegenerative disease. However, the discovery of multiple pathogenic mutations in the *tau* gene of several FTDP-17 families provided direct unequivocal evidence that tau abnormalities cause neurodegenerative disease. The FTDP-17 mutations (i.e., missense substitutions, in-frame deletion, intronic substitutions) occur in exons and introns of the *tau* gene (Clark et al., 1998; Hutton et al., 1998; Iijima et al., 1999; Poorkaj et al., 1998; Spillantini et al., 1998b; D'Souza et al., 1999; Rizzu et al., 1999), and they may cause FTDP-17 by altering the functions or levels of specific tau isoforms in the CNS (Hong et al., 1998; Hutton et al., 1998; D'Souza et al., 1999). For example, intronic substitutions and some missense mutations alter splicing and increase mRNAs that encode four MT-binding repeat tau (4R-tau), as well as the corresponding proteins in the CNS, and this is associated with the selective aggregation of 4R-tau into filamentous inclusions and the degeneration of affected brain regions (Hong et al., 1998; D'Souza et al., 1999). Thus, we hypothesize that neurodegenerative disease can result from altered expression levels of normal tau isoforms.

To test this hypothesis, we generated transgenic (Tg) mice that overexpressed the shortest human brain tau isoform ("fetal tau") in CNS neurons, and we report that these Tg mice develop progressive age-dependent accumulations of intraneuronal filamentous inclusions, accompanied by neurodegeneration, gliosis, and tau protein abnormalities. Since overexpression of normal tau in these Tg mice causes a neurodegenerative disease that partially recapitulates human tauopathies, these mice will be useful in studies to elucidate mechanisms of brain degeneration in tauopathies.

Results

Generation of Tg Mice that Overexpress the Shortest Human Tau Isoform

To generate Tg mice expressing human tau, a cDNA corresponding to the shortest human brain tau isoform (T44, also known as fetal tau) was cloned into an expression plasmid, MoPrP.Xho, containing the promoter as

‡To whom correspondence should be addressed (e-mail: vmylee@mail.med.upenn.edu).

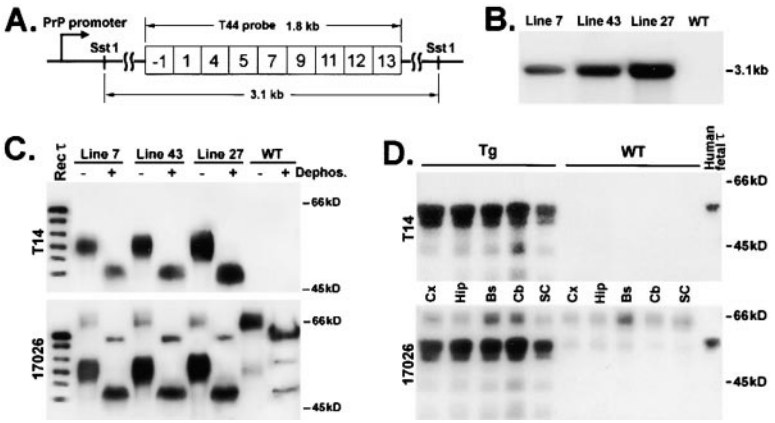

Figure 1. Tg Mice Expressing the Shortest Human Brain Tau Generated with the Murine PrP Promoter

(A) Schematic showing structure of the cDNA transgene used to make tau Tg mice (not drawn to scale). Numbered boxes represent exons contained in the human fetal tau cDNA (T44 or fetal tau).

(B) Southern blot analysis of the transgene in Tg mice from lines 7, 43, and 27 by probing SstI-digested tail DNA with a 1.8 kb BamHI–KpnI T44 fragment. Semiquantitatively, line 27 has the highest transgene level, and line 7 has the lowest.

(C) Western blot analysis of tau expression in the cortices of Tg mice. Dephosphorylated (+) and nondephosphorylated (−) samples, along with a mixture of six recombinant human tau proteins, were resolved on 7.5% SDS–PAGE and blotted with T14 and 17026. Equal amounts of total protein (15 μg) were loaded for the Tg mice (line 7 and line 43, 3 months old; line 27, 9 weeks old), and 135 μg was loaded for the wt mouse (3 months old). The overexpression levels in each line were calculated by quantitating the nondephosphorylated tau bands recognized by 17026.

(D) Western blot analysis of regional expression of tau in the cerebral cortex (Cx), hippocampus (Hip), brainstem (Bs), cerebellum (Cb), and spinal cord (SC) of line 7 Tg and wt mice (6 months old). Equal amounts (15 μg) of mouse samples and an aliquot of autopsy-derived human fetal tau were loaded on each gel.

well as 5′ intronic and 3′ untranslated sequences of the *murine prion protein* (*PrP*) gene (Figure 1A). This vector was used here because it enables relatively high levels of transgene expression in CNS neurons (Borchelt et al., 1996). Tg mice were identified by Southern blot analysis using a human T44 cDNA probe, which detected the transgene as a 3.1 kb band from SstI-digested genomic DNA obtained from tail samples (Figures 1A and 1B).

Three stable Tg lines were established that variably overexpressed human tau, as demonstrated by quantitative Western blot analysis of whole-brain extracts from heterozygous Tg mice. Figure 1C illustrates representative Western blots produced by loading equal amounts of total protein from Tg mice and 9-fold more protein from a wild-type (wt) littermate control, before and after dephosphorylation, into adjacent lanes of a gel followed by electrophoresis and protein transfer to blot membranes. These data show that tau proteins from all three Tg mouse lines, but not from the wt mouse, are detected by T14, a human tau-specific monoclonal antibody (mAb), and that the dephosphorylated tau bands from the Tg mice align with recombinant fetal human tau. Using a polyclonal antibody (17026) that recognizes human and mouse tau in quantitative Western blot studies, we showed that the heterozygous Tg mouse lines 7, 43, and 27 overexpressed tau proteins at levels that were approximately 5-, 10-, and 15-fold higher, respectively, than endogenous mouse tau. Figure 1D demonstrates that the expression levels of Tg tau varied in different CNS regions, as revealed by Western blot studies conducted on Tg line 7 with antibodies T14 and 17026. For example, neocortex, hippocampus, brainstem, and cerebellum express comparable levels of Tg tau, but spinal cord expresses ~60% of those seen in these regions.

Although the heterozygous line 27 mice had the highest levels of Tg tau, they were not viable beyond 3 months, and homozygous mice generated from each of the three lines died in utero or within 3 months postnatal. Therefore, the studies described below were conducted on 1- to 12-month-old heterozygous Tg mice from lines 7 and 43.

Tau Tg Mice Acquire CNS Tau Inclusions Similar to Human Tauopathies

Tg mice and their wt littermates from lines 7 and 43, between 1 and 12 months of age, were subjected to histological studies. Paraffin-embedded coronal brain sections and transverse spinal cord sections were stained with T14 to determine the regional and cellular distribution of Tg tau. These studies demonstrated widespread expression of human tau in neurons and their processes throughout the CNS of the Tg but not the wt mice, and the intensity of tau immunoreactivity in the Tg mice remained constant at all ages examined (Figures 2 and 3).

In Tg mouse spinal cords, T14-positive spheroidal intraneuronal inclusions were observed at 1 month, and the size and number of these inclusions increased for up to 6–9 months, but they decreased in abundance by 12 months (Figures 2A–2C). Notably, many vacuolar lesions of the same size or larger than the inclusions were also observed in the older Tg mice (Figure 2C), which may reflect the degeneration of affected axons. The inclusions were about the size of medium-to-large spinal cord neurons, and some appeared to arise within proximal axons of spinal cord neurons. Although they occurred in gray and white matter at all spinal cord levels, the inclusions were most frequent at the gray–white junction.

Spinal cord sections were probed with a panel of antibodies to tau and other neuronal cytoskeletal proteins, and the inclusions were immunostained by an antibody commonly used to detect tau protein found in PHFs (i.e., Alz50; Figure 2D) and other hyperphosphorylated PHF-tau epitopes, including PHF1 (phosphoserine 396 and 404, numbering according to the largest human brain tau), PHF6 (phosphothreonine 231), T3P (phosphoserine 396), AT8 (phosphoserine 202 and 205), AT270 (phosphothreonine 181), and 12E8 (phosphoserine 262) (data not shown). Therefore, these lesions contain hyperphosphorylated tau similar to PHF-tau. Significantly, these inclusions were also stained strongly with antibodies to the low- (NFL), middle- (NFM), and high- (NFH) molecular mass NF proteins (Figures 2F–2H and 2K).

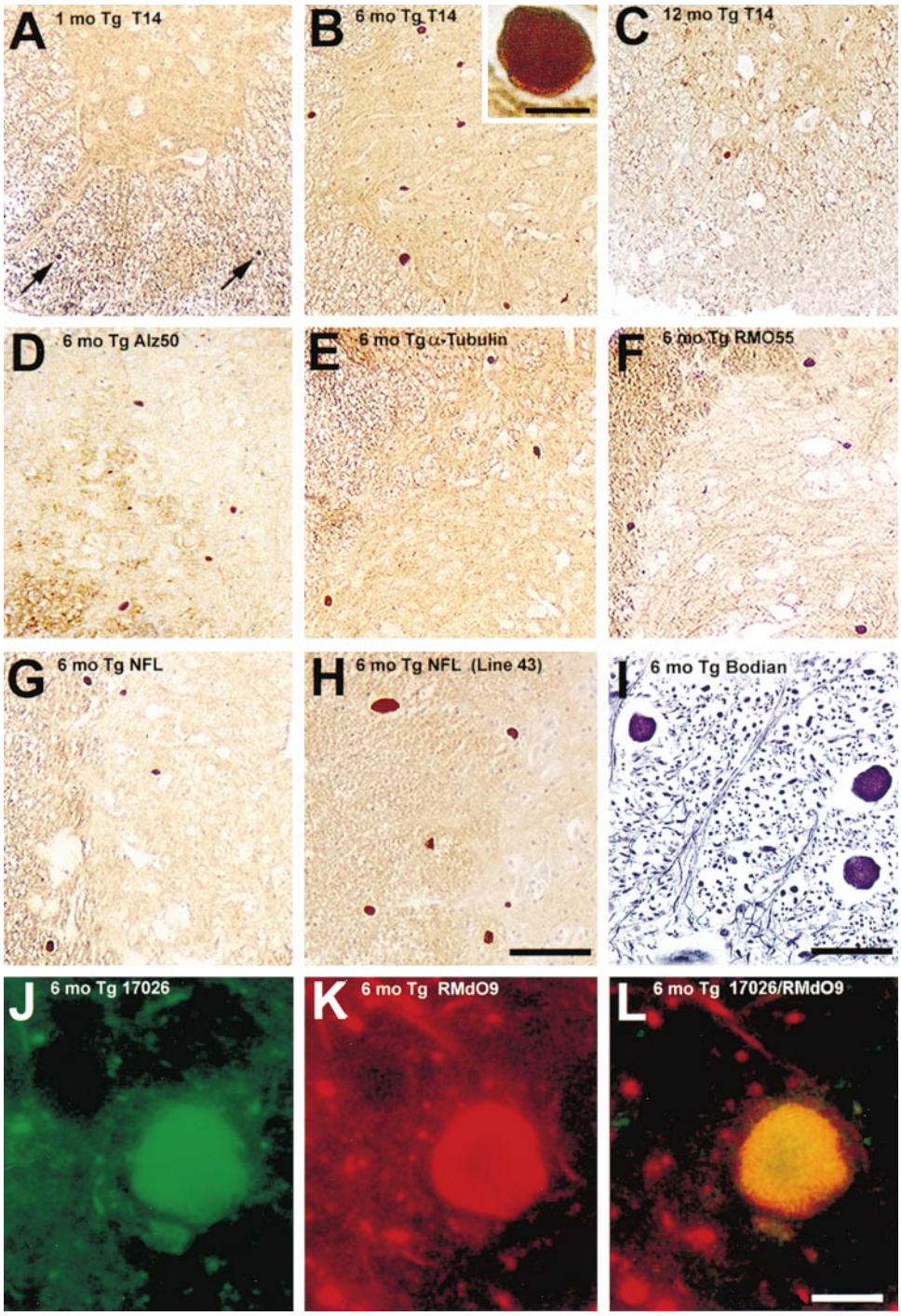

Figure 2. Tau Tg Mice Developed Tau-Rich Inclusions in the Spinal Cord

(A–C) Spheroidal intraneuronal inclusions in spinal cord sections of 1-, 6-, and 12-month-old Tg mice stained with T14, which appeared as early as 1 month of age (arrows) and peaked at 6–9 months but decreased at 12 months.

(D–I) The inclusions were stained positive with Alz50 (D), α-tubulin (E), and antibodies against NF proteins (F–H), as well as by Bodian silver method (I). The inclusions seen in line 43 Tg mice (H) were larger in size and appeared earlier than those in line 7.

(J–L) Double-labeled indirect immunofluorescence of the spinal cord inclusions from a 6-month-old Tg mouse. Green, 17026 (J); red, RMdO9 (K); and double channels (L).

Scale bar, 100 μm (A–H); 10 μm ([B], inset); 30 μm (I); and 10 μm (J–L).

Both phosphorylated and nonphosphorylated NFM and NFH were observed in these lesions. Indirect immunofluorescence double labeling with antibodies 17026 and RMdO9 confirmed the colocalization of tau and NFs in these inclusions (Figures 2J–2L). In addition, anti-tubulin antibodies immunostained these inclusions (Figure 2E).

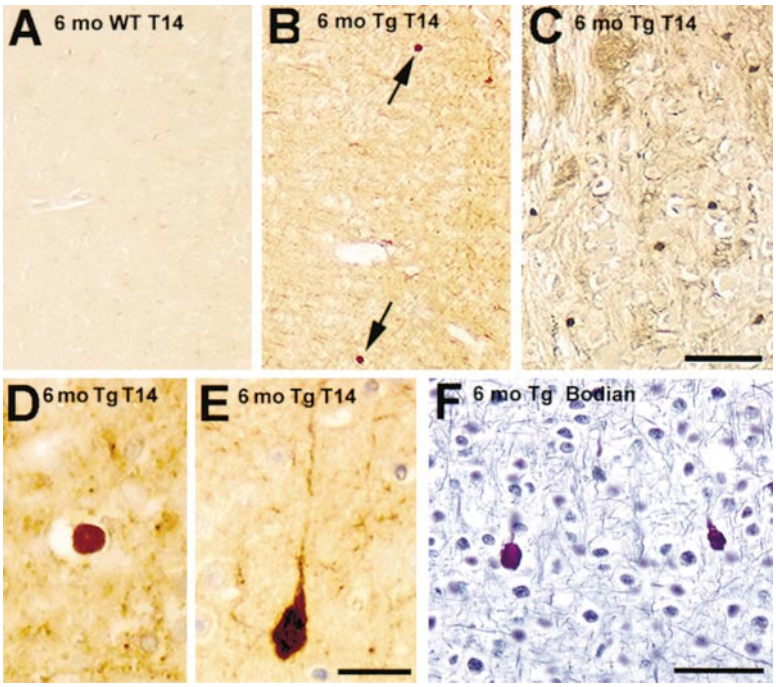

Figure 3. Tau Tg Mice Developed Tau-Rich Inclusions in Cortical and Brainstem Neurons

Cerebral cortices of 6-month-old wt (A) and Tg (B) mice stained with T14. Arrows in (B) indicate small, tau-positive intraneuronal lesions. Similar lesions were also observed in pontine neurons of Tg mice (C). The cortical lesions occurred either in proximal axons (D) or in somatodendritic domains (E) of neurons. Brainstem inclusions are also stained by the Bodian silver method (F). Scale bar, 100 μm (A–C); 20 μm (D and E); and 30 μm (F).

In the brains of the Tg mice, tau-positive intraneuronal aggregates were also detected, but they were smaller and appeared later than the spinal cord inclusions. They were first seen in the pontine neurons of 1-month-old animals and emerged in the cerebral cortex at about 6 months of age (Figure 3). The immunohistochemical profile of these brain aggregates was similar to that of the spinal cord lesions, i.e., they contained hyperphosphorylated tau, all three NF subunits, and tubulin epitopes (data not shown). However, the morphological features of these inclusions indicates that some are variants of the spinal cord axonal lesions (Figure 3D), but others occur in the somatodentritic compartment of cortical neurons and resemble NFTs and dystrophic neurites (Figure 3E). Notably, the brain and spinal cord inclusions were positively stained by the Bodian silver method (Figures 2I and 3F), similar to human NFTs, but were thioflavine S negative, and they were not stained by antibodies to α-internexin, peripherin, ubiquitin, or synucleins (data not shown).

Line 43 expressed higher levels of human tau than line 7, and similar tau-rich inclusions were also observed in the spinal cord and the brain in an age-dependent manner (Figure 2H), but they were larger and more abundant than in line 7. For example, we found that in the spinal cord of 6-month-old animals, line 43 expresses twice as many tau inclusions as line 7. These results indicate that the accumulation of these tau-rich lesions in the tau Tg mice is transgene dose dependent as well as age dependent.

Transmission electron microscopy (EM) studies of these inclusions (Figure 4) revealed masses of tightly packed aggregates of randomly arranged 10–20 nm straight filaments in the myelinated spinal cord axons of Tg (Figures 4B and 4C) but not wt (Figure 4A) mice. These aggregates were found in ≈30% of myelinated and unmyelinated axons ranging from 200 nm to 20 μm in diameter, and some inclusions almost completely filled the axon. Mitochondria were trapped within occasional aggregates (Figure 4C). Immuno-EM studies showed that the filaments were immunolabeled by antibodies to tau, NFs, and tubulin (Figures 4D–4F).

Since the argyrophilic filamentous lesions of our Tg mice are concentrated in the spinal cord and brainstem, and since tau-positive NFTs and dystrophic neurites are found in the spinal cord of some ALS/PDC patients and in the brainstem of PSP and FTDP-17 patients, we directly compared the tau inclusions in spinal cord of ALS/PDC and brainstems of PSP and FDTP-17 with those in our Tg mice, and we found that they were similar (see Figures 5A–5D, and compare Figures 3C–3E with Figures 5B–5D). Significantly, in the ALS/PDC spinal cord, NF immunoreactivity colocalized with tau in many of the inclusions (compare Figures 5E–5G with Figures 2J–2L). These data, taken together with the findings described above, suggest that these tau Tg mice develop a neurodegenerative disease that recapitulates the hallmark lesions of human tauopathies.

Insoluble Tau Protein Progressively Accumulates in the CNS of Tau Tg Mice

To determine whether tau became insoluble in the tau Tg mice with age and disease progression, as in human tauopathies, we analyzed the solubility of tau protein by extracting brain and spinal cord samples using buffers with increasing extraction strengths. As shown in Figure 6, the spinal cord and brain samples from 1-, 3-, 6-, and 9-month-old line 7 Tg and wt mice were sequentially extracted with reassembly buffer (RAB), radioimmunoprecipitation assay (RIPA) buffer, and 70% formic acid (FA). The three fractions were then analyzed by quantitative Western blotting with antibody 17026. In the wt mice, about 90% of endogenous mouse tau in both the brain and the spinal cord was largely RAB-soluble and

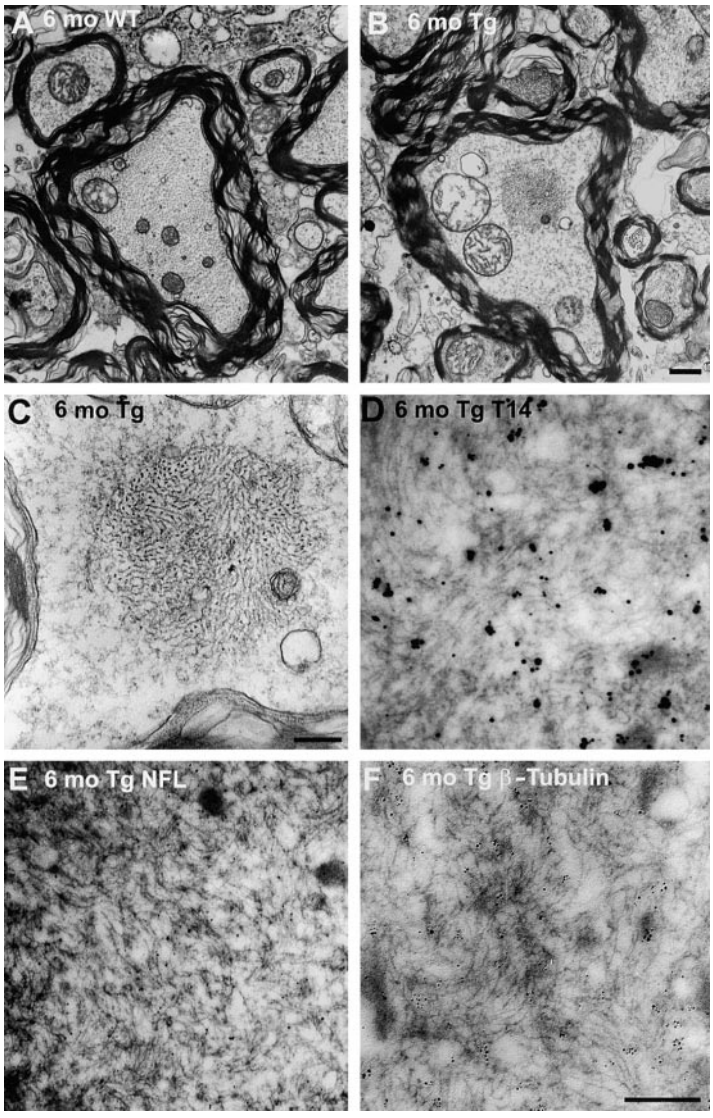

Figure 4. Tau-Rich Inclusions in Proximal Axons Contained Straight Filaments

(A) NFs evenly distributed in a spinal cord–myelinated axon of a wt mouse.

(B and C) Masses of tightly packed disorganized filamentous aggregates in a spinal cord axon of a 6-month-old Tg mouse.

(D–F) Postembedding immuno-EM labeled the aggregates with T14 (D), NFL (E), and anti-β-tubulin (F) antibodies. Note that silver enhancement was performed for T14 staining.

Scale bar, 500 nm (A and B); 300 nm (C); and 200 nm (D–F).

no immunoreactivity was detected in the FA-soluble fraction. In the Tg mice, although the RAB-soluble tau remained relatively constant at around 75%–80% with increasing age, RAB-insoluble tau represented by the RIPA and FA fractions progressively accumulated in both the brain and the spinal cord. For example, RIPA-soluble tau in brain increased from about 17% at 1 month to about 25% at 9 months, and FA-soluble tau in spinal cord increased from about 0.4% to about 1.8% over the same time period. The accumulated RAB-insoluble tau was mainly Tg tau, and the time course of accumulation correlated with the emergence of tau pathology in the Tg mice. In addition, RAB-insoluble tau, especially the FA fraction, was more pronounced in spinal cord than brain, consistent with more abundant tau aggregates in the spinal cord.

The Phosphorylation State of Tau in Tg Mice Recapitulates that of PHF-Tau

To determine whether tau proteins in tau Tg mice possessed the same hyperphosphorylated epitopes as PHF-tau, we performed Western blot analysis of soluble and insoluble tau extracted from the cerebral cortex of Tg mice. As shown in Figure 7, phosphorylation-independent antibody 17026 recognized human PHF-tau, adult normal tau, and fetal tau, as well as both soluble and insoluble mouse endogenous tau and Tg tau. Similarly, T14 recognized all but the mouse tau sample. mAb T1 (specific for a tau epitope that is not phosphorylated at amino acids 189–207) did not recognize PHF-tau but was immunoreactive with human adult normal tau, fetal tau, and both soluble and insoluble Tg tau. This indicates that tau from the Tg mice is partially dephosphorylated at the T1 epitope. However, several phosphorylation-dependent antibodies that reacted with PHF-tau and fetal tau, but not with normal adult tau, also recognized both soluble and insoluble tau from the Tg mice. These antibodies include PHF1 (phosphoserine 396 and 404), T3P (phosphoserine 396), PHF6 (phosphothreonine 231), AT8 (phosphoserine 202 and 205), AT270 (phosphothreonine 181), and 12E8 (phosphoserine 262). Therefore, the phosphorylation state of Tg tau recapitulates that of

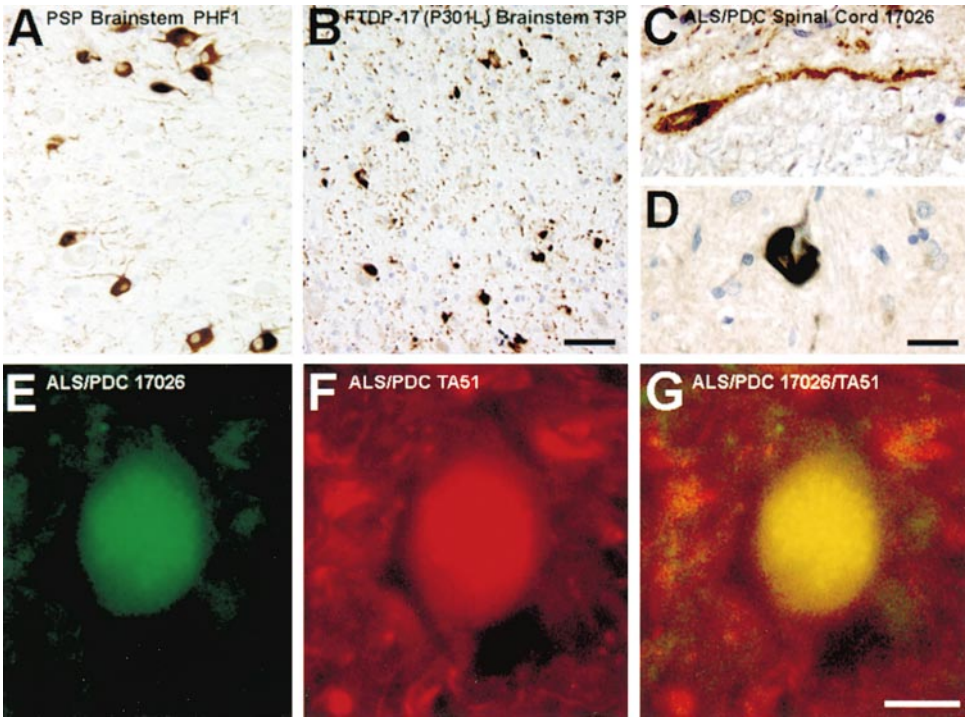

Figure 5. Neurofibrillary Lesions in Brainstem and Spinal Cord of Neurodegenerative Tauopathies

(A–D) Numerous neurofibrillary lesions in brainstem sections stained with PHF1 in a PSP (A) and T3P in an FTDP-17 with the P301L tau mutation (B) case. Tau-positive dystrophic neurites (C) and NFTs (D) also were stained with 17026 on a spinal cord section of ALS/PDC.

(E–G) Double-labeled indirect immunofluorescence with antibodies 17026 and TA51 indicated the colocalization of tau and NF epitopes in the spinal cord lesions of ALS/PDC.

Scale bar, 40 μm (A and B); 20 μm (C and D); and 10 μm (E–G).

PHF-tau found in human tauopathies and human fetal tau but is different from that of normal adult human tau.

Tau Tg Mice Develop Profound Astrocytosis, Reduced Fast Axonal Transport, and Progressive Motor Weakness Contemporaneous with Axonal Degeneration

To examine the pathological consequences of the accumulation of hyperphosphorylated tau as filamentous aggregates in the CNS of the tau Tg mice, brain and spinal cord sections were stained with a mAb specific for glial fibrillary acidic protein (GFAP) to detect astrocytosis reactive to neuronal damage. In the Tg but not the wt mice, numerous reactive astrocytes were immunostained in both the brain and the spinal cord (data not shown), indicative of profound gliosis and neuronal damage. Further, the astrocytosis was almost undetectable at 1 month of age but progressed thereafter with age.

Since inclusions in the proximal axons of affected neurons could cause disease by damaging axons, we examined the morphology of spinal cord ventral root axons. In Figure 8A, semithin section micrographs show

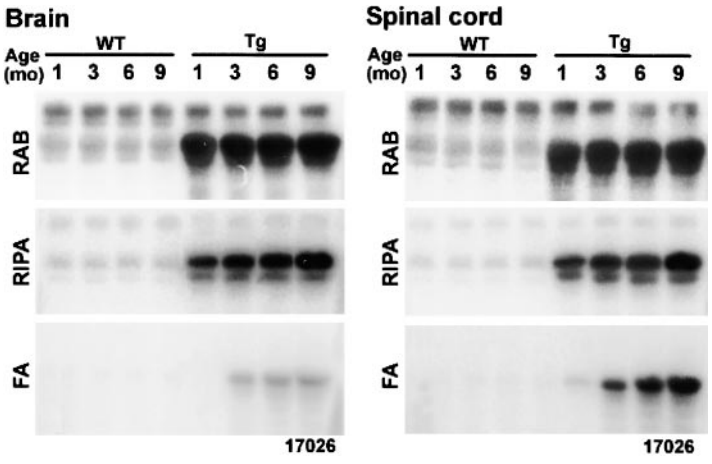

Figure 6. Insoluble Tau Protein Progressively Accumulated in the CNS of Tau Tg Mice

Neocortical and spinal cord tissues of 1-, 3-, 6-, and 9-month-old Tg and wt mice were sequentially extracted with RAB Hi-Salt, RIPA buffer, and 70% FA, and the tau levels were determined by quantitative Western blot analysis with 17026. RAB-insoluble tau, represented by the RIPA and FA fractions, progressively accumulated in both the brain and the spinal cord of the Tg mice but not in the wt mice.

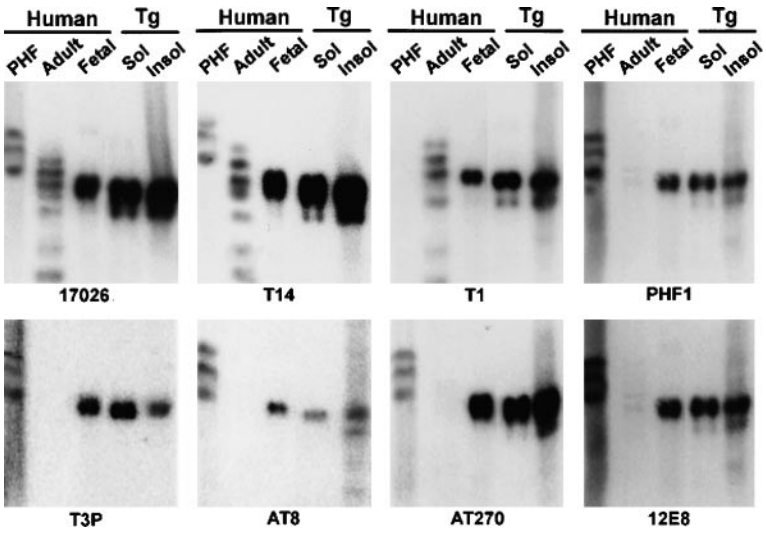

Figure 7. The Phosphorylation State of Tg Tau Recapitulated that of PHF-Tau

AD PHF-tau, autopsy-derived normal human adult tau, and autopsy-derived human fetal tau samples were run along with neocortical soluble and insoluble tau from a 6-month-old Tg mouse. Antibodies 17026 and T14 reacted with tau proteins, regardless of phosphorylation. Non-phosphorylation-dependent antibody T1 did not recognize PHF-tau. Phosphorylation-dependent antibodies PHF1, T3P, AT8, AT270, and 12E8 did not react with normal adult tau but recognized PHF-tau and fetal tau, as well as both soluble and insoluble tau from the Tg mouse.

the normal lumbar 5 (L5) ventral root of wt mouse, containing many large- and small-sized myelinated axons. By contrast, the ventral root of a 6-month-old Tg mouse primarily contained irregularly shaped axons (Figure 8B), and at 12 months of age, the endoneurial space appeared to increase (Figure 8C), consistent with the removal of degenerated axons in these nerves. Evidence of axonal degeneration also came from comparing axon

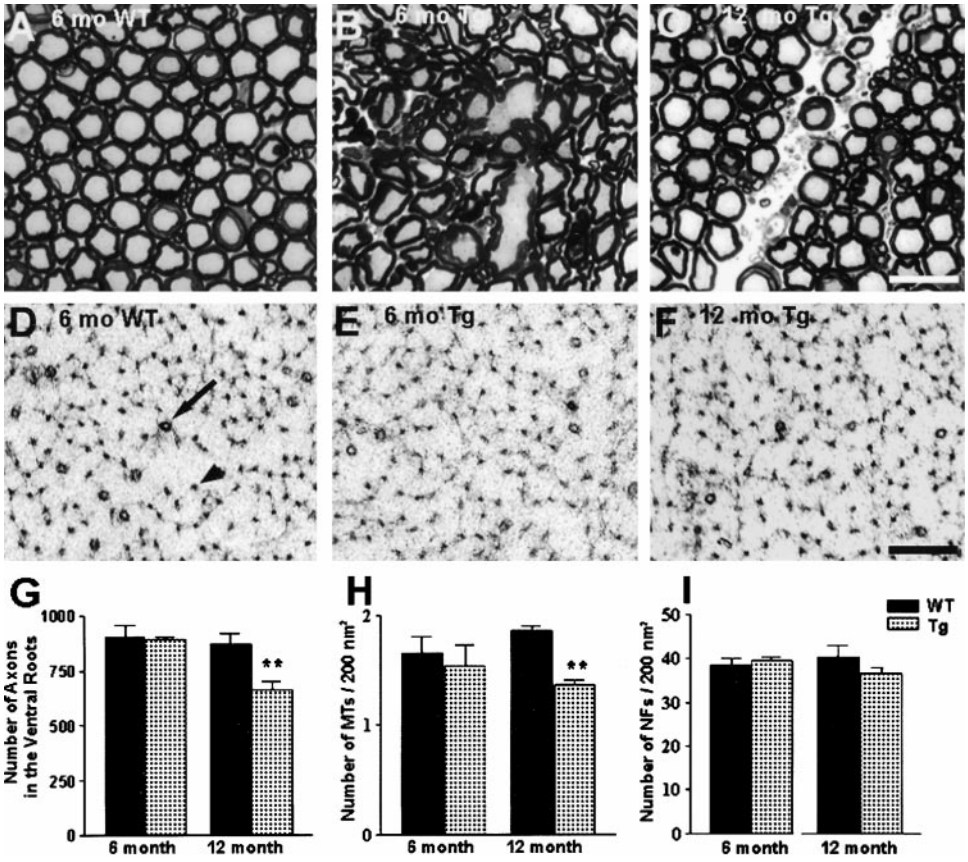

Figure 8. Axonal Degeneration in the Spinal Cord Ventral Roots and Reduction of Axonal MTs in Tau Tg Mice

A semithin section micrograph shows the L5 ventral root of a 6-month-old wt mouse, which contains many large- and small-sized myelinated axons tightly packed and evenly distributed (A). In 6-month-old Tg mice, the ventral root axons are irregularly shaped (B), and by 12 months of age a prominent endoneurial space is found in Tg mice (C). MTs (arrow) and NFs (arrowhead) in the ventral root axons were visualized by EM micrographs (D–F). Quantification of ventral root axon numbers demonstrates a 20% reduction ($n = 3$) in the Tg mice relative to their wt littermates (G). A significant reduction in the MT density was observed in the 12-month-old Tg mice (H), and there was no significant difference in NF density in the Tg mice relative to the wt mice (I). Scale bar, 20 μm (A) and 200 nm (B). Double asterisk, $p < 0.01$.

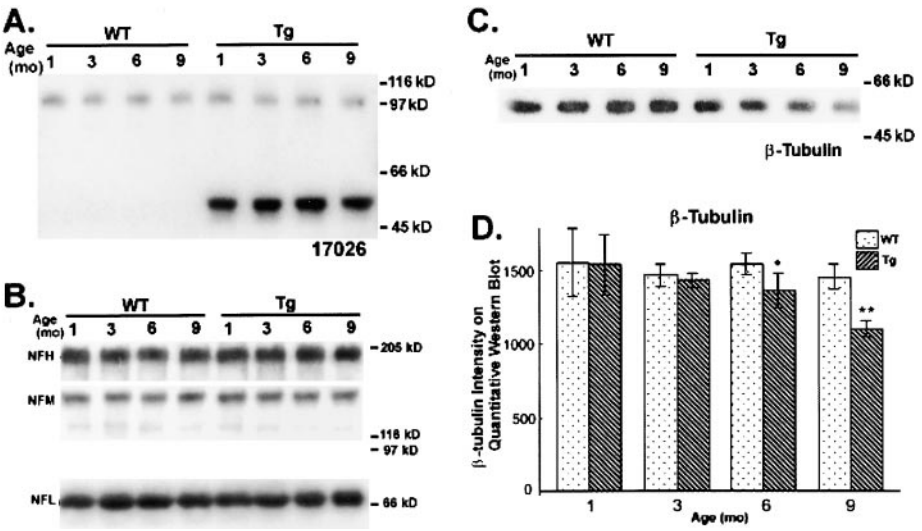

Figure 9. Tubulin Level Was Decreased in the Sciatic Nerve of Tau Tg Mice

Western blots showing tau (A), NF (B), and β-tubulin (C) levels in the sciatic nerve of 1-, 3-, 6-, and 9-month-old wt and Tg mice. The Tg tau levels (A) were comparable in different ages. Note the peripheral nervous system tau isoform ("big tau") as the upper bands in the tau blot (A). There was no significant difference in the NF protein level in the Tg mice relative to the wt mice (B). However, a progressive decrease in β-tubulin levels was detected in the Tg mice but not in the wt mice (C and D); $n = 3$; asterisk, $p < 0.05$; double asterisk, $p < 0.01$.

numbers in L5 ventral roots of Tg and wt mice, based on semithin section micrographs. Although at 6 months of age the number of axons in the Tg mice was comparable to that measured in of age-matched wt mice, a 20% decrease was seen in 12-month-old Tg mice, relative to their wt counterparts (Figure 8G). We also determined the densities of NFs and MTs in the L5 ventral root axons in these mice (Figures 8D–8F). Interestingly, despite a significant reduction of MT density in the 12-month-old Tg mice, the NF density remained unchanged when compared with age-matched wt mice (Figures 8H–8I). This finding correlated with the biochemical analysis of β-tubulin and NF subunits in the proximal sciatic nerve, which showed a progressive decrease in β-tubulin level in the Tg mice and relatively constant levels of NF subunits (Figure 9).

To assess whether or not the neuropathology in ventral roots of 12-month-old tau Tg mice compromised axonal transport, we measured radiolabeled proteins transported in the fast component following microinjection of [^{35}S]methionine into the L5 ventral horn of tau Tg and age-matched wt mice, and this showed retarded fast axonal transport of radiolabeled proteins in the tau TG mice (Figure 10A). The greatest differences in the amounts of transported radiolabeled proteins appeared around the 4 mm segment, where almost twice as many radiolabeled proteins were detected in wt compared with tau TG mice (Figure 10B).

In addition to acquiring the spinal cord pathologies described above, the tau Tg mice also developed progressive motor weakness, as demonstrated by their impaired ability to stand on a slanted surface and by retraction of their hindlimbs when lifted by their tails (data not shown). These impairments may explain the fact that the Tg mice weighed about 30%–40% less than age-matched wt littermates.

Discussion

Our study provides compelling evidence that the overexpression of normal tau protein in Tg mice causes a CNS neurodegenerative tauopathy that recapitulates key aspects of human tauopathies, such as ALS/PDC and PSP, as well as some FTDP-17 syndromes. For example, we observed a progressive, age-dependent accumulation of argyrophilic, tau-immunoreactive inclusions in neurons of spinal cord, brainstem, and neocortex, similar to human tauopathies. Since the inclusions in the Tg mice were most abundant in spinal cord neurons, the tauopathy in these mice most closely resembles ALS/PDC, wherein tangles are abundant in spinal cord neurons (Hirano et al., 1961; Matsumoto et al., 1990). Significantly, ALS/PDC patients who present with motor weaknesses do so about a decade earlier than those who present with parkinsonism and dementia. Thus, the accumulation of tau aggregates in the brains of our Tg mice later than in spinal cord mirrors disease progression in ALS/PDC patients who present with motor weakness. Moreover, as shown here and reported earlier, these tau tangles also are immunostained by antibodies to NF proteins and tubulin (Shankar et al., 1989), as are the inclusions in our Tg mice. Finally, ALS/PDC is associated with a progressive motor weakness similar to that observed in the Tg mice.

Although the distribution of the tau pathology in our mice most closely resembles that found in ALS/PDC and PSP, as well as in some FTDP-17 syndromes, these filamentous tau aggregates share many characteristics with authentic NFTs in AD and other tauopathies. First, like highly insoluble PHF-tau, in AD NFTs (Bramblett et al., 1992) a substantial fraction of tau proteins from the Tg mice is extracted only with RIPA and FA, despite the fact that normal tau is an extremely soluble protein.

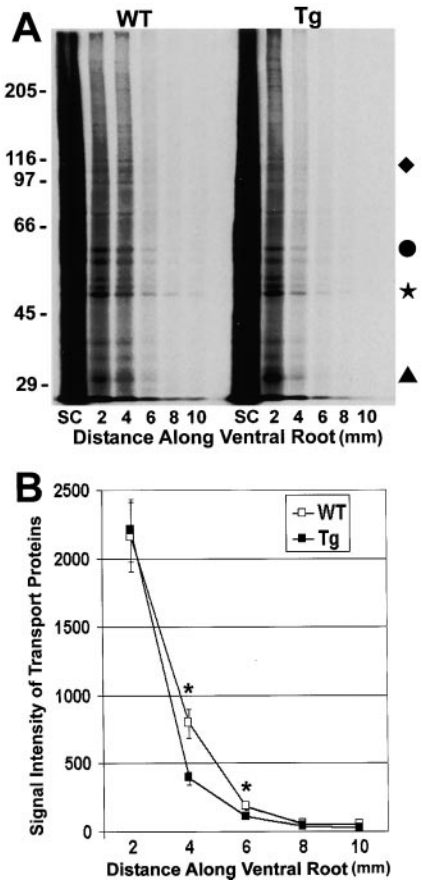

Figure 10. Orthograde Fast Axonal Transport Is Reduced in the Ventral Root Axons of the Tau Tg Mice

SDS–PAGE analysis shows retardation in the L5 ventral roots of the spinal cord in the tau Tg mice compared with wt mice. Fluorograph highlights a retardation in the fast transport of several proteins (closed diamond, circle, star, and triangle) in the 12-month-old Tg mice (A). The graph in (B) illustrates quantitative measurements of proteins conveyed by fast axonal transport in tau Tg and wt mice (average of six nerves from groups of three animals). The fast transport of several proteins is retarded in the 12-month-old Tg mice compared with wt mice (B). Asterisk, $p < 0.05$.

Second, the amount of insoluble tau protein progressively accumulates with age and disease progression in the Tg mice, similar to AD and other tauopathies. Third, PHF-tau proteins in human NFTs are hyperphosphorylated, and so is soluble and insoluble tau recovered from Tg mice (Lee et al., 1991; Matsuo et al., 1994). Fourth, although AD NFTs contain mostly PHFs, straight filaments similar to those found in the inclusions of the Tg mice are also present (Goedert et al., 1997). Finally, in addition to ALS/PDC, NF protein immunoreactivity also occurs in the NFTs of AD, PSP, and other tauopathies (Nakazato et al., 1984; Perry et al., 1985; Shankar et al., 1989; Schmidt et al., 1990, 1991).

Despite similarities found between the tau aggregates in our Tg mice and those of other tauopathies, the tau inclusions in the Tg mice are not identical to AD NFTs, which composed all of six tau isoforms, while the Tg tau proteins do not contain all six tau isoforms. In this regard, the filamentous Tg tau inclusions perhaps more closely resemble Pick bodies found in Pick's disease, since Pick bodies are composed almost exclusively of 3R-tau isoforms. One notable difference, however, is that all three brain 3R-tau isoforms are found in Pick bodies, whereas only the fetal 3R-tau isoform is present in the tau aggregates in the Tg mice. Nevertheless, it is noteworthy that insoluble tau tangles composed of all six tau isoforms (as seen in AD and ALS/PDC), or predominantly of 4R-tau isoforms (as detected in PSP) or 3R-tau (as found in Pick's disease), have been reported, and recent studies of FTDP-17 and other familial tauopathies suggest that tau tangles composed of different ratios of the six alternatively spliced tau isoforms exist in different tauopathies (Hong et al., 1998; Hutton et al., 1998; Spillantini et al., 1998b; D'Souza et al., 1999). Thus, multiple mechanisms can perturb *tau* gene function, resulting in the formation of tau tangles with different tau isoforms.

Since the accumulation of filamentous tau inclusions in spinal cord neurons was associated with the degeneration of ventral root axons in the tau Tg mice, we hypothesize that this reflects a gain of toxic function by the overexpressed tau, and several lines of evidence support this hypothesis. First, previously described tau Tg mice that expressed lower levels (<2-fold) of tau protein did not develop filamentous tau inclusions or neurodegeneration (Goetz et al., 1995; Brion et al., 1999). Second, we observed a Tg tau dose-dependent increase in the size and number of tau aggregates in our two lines of Tg mice. Thus, one plausible explanation to account for the axonal degeneration in these Tg mice is a gain of toxic function by the excess tau proteins that cannot bind MTs, aggregate in the neuronal cytoplasm, block axonal transport, and lead to the degeneration of affected axons.

The reduced numbers of MTs and the reduced levels of tubulin, but not NFs or NF proteins, in the remaining axons of the degenerating ventral roots also imply a loss of the MT-stabilizing function of tau. Since our data showed that the level of endogenous mouse tau (i.e., only 4R-tau) is not altered in the tau Tg mice, the endogenous mouse tau should be sufficient to stabilize MTs in the Tg mice. However, overexpressed human tau could aggregate with endogenous mouse tau, leading to progressive insolubility and hyperphosphorylation of both human and mouse tau in the Tg mice. This could impair endogenous mouse tau from performing an MT-stabilizing function. Indeed, the observed reduction in fast axonal transport in 12-month-old Tg mice is consistent with a loss of MT function, although the loss of axons in the Tg mice may contribute to this. Based on indirect evidence from studies of human tauopathies, we and others have proposed that both gains of toxic functions and losses of normal tau functions could be involved mechanistically in causing neurodegenerative disease (Hong et al., 1998; Hutton et al., 1998; D'Souza et al., 1999), and the data presented here support both of these mechanistic hypotheses.

Although a dose effect of the transgene is observed in two different Tg mouse lines, the distribution of the tau-rich lesions within the CNS is not completely dependent upon the expression levels across the different regions. For example, spinal cord expresses less Tg tau than brain, but more abundant and larger inclusions

accumulate earlier in spinal cord neurons than in the other brain regions. This could be explained by the metabolic differences among diverse types of neurons, and excess tau may aggregate at a lower concentration in spinal cord neurons under the influence of local factors or chaperones, such as high concentrations of NF proteins. Similarly, the selective distribution of tau pathology in different human tauopathies is likely due to other as yet unidentified local vulnerability factors. Indeed, the findings described here parallel the well-known but enigmatic "selective vulnerability" that is a constant feature of most human neurodegenerative diseases and Tg mouse models thereof (Tu et al., 1997). Similar to all animal models of human diseases, the Tg tau mice described here do not fully recapitulate every feature of a human neurodegenerative tauopathy, but this Tg model exhibits the key neuropathological features that define this class of CNS disorders. Therefore, these mice will be useful in studies designed to further elucidate mechanisms leading to the formation of tau pathology and the selective degeneration of neurons in FTDP-17, PSP, ALS/PDC, AD, Pick's disease, and related tauopathies.

Experimental Procedures

Generation of Tau Tg Mice

A cDNA construct of the shortest human brain tau isoform (T44) was cloned into the MoPrP.Xho expression vector at the XhoI site. A 15 kb NotI fragment containing T44, the PrP promoter, together with its 3′ untranslated sequences, was used as the transgene to create tau Tg mice on a B6D2/F1 background. Genomic DNA samples were isolated from mouse tails with the Puregene (Gentra Systems) DNA isolation kit. Potential founders were identified by Southern blot analysis with a ^{32}P-labeled T44 probe. Three stable Tg lines (lines 7, 27, and 43) were established, and Tg and wt offspring were identified by Southern blot analysis of tail DNA.

Western Blot Analysis of Tau Expressed in the CNS of wt and Tg Mice

To estimate tau expression levels in different Tg lines and in the diverse CNS regions of line 7 Tg mice, tissues were carefully dissected after mice were lethally anesthetized. The tissues were homogenized in 2 ml/g of ice-cold RAB Hi-Salt buffer (0.1 M morpholineethanesulfonic acid (MES), 1 mM EGTA, 0.5 mM $MgSO_4$, 0.75 M NaCl, 0.02 M NaF, 1 mM phenylmethylsulfonyl fluoride, and 0.1% protease inhibitor cocktail [100 μg/ml each of pepstatin A, leupeptin, N-tosyl-L-phenylalanyl chloromethyl ketone, N-tosyl-lysine chloromethyl ketone, and soybean trypsin inhibitor, and 100 mM EDTA (pH 7.0)]) and centrifuged at 50,000 × g for 40 min at 4°C in the Beckman TL-100 ultracentrifuge. The supernatants were boiled for 5 min, chilled on ice for 5 min, and recentrifuged at 10,000 × g for 20 min at 4°C. Protein concentration was then determined for the second supernatants with the BCA assay kit (Pierce). To prepare dephosphorylated tau, an aliquot of the supernatant was incubated with *Escherichia coli* alkaline phosphatase (Sigma) at 37°C overnight as described (Hong et al., 1998). Equal amounts (15 μg) of nondephosphorylated and dephosphorylated samples were subsequently resolved on 7.5% SDS–PAGE gels and transferred onto nitrocellulose membranes. Quantitative Western blot was performed by using ^{125}I-labeled goat anti-mouse immunoglobulin G (IgG) or ^{125}I-labeled Protein A (NEN) as secondary antibodies. Recombinant proteins of the six human brain tau isoforms and human fetal tau were made as previously described (Goedert and Jakes, 1990).

Immunohistochemical and Histochemical Studies

Animals were perfused transcardially with 15 ml of phosphate-buffered saline (PBS) followed by 15 ml of 70% isotonic ethanol after being lethally anesthetized. The brains and spinal cords were removed and continuously fixed overnight by immersion in 70% isotonic ethanol. Paraffin-embedded sections were prepared and probed by immunohistochemistry as described (Tu et al., 1995). Double-label indirect immunofluorescence was performed with anti-tau and anti-NF antibodies and detected by FITC-conjugated donkey anti-rabbit IgG and Texas Red–conjugated donkey anti-mouse IgG (Jackson Laboratories), respectively. Hematoxylin and eosin, thioflavine S, and Bodian silver staining methods also were used to characterize the neuropathology in Tg and wt mice. Light and fluorescent microscopy were performed with a Nikon Microphot-FXA microscope system. At least three Tg and one wt mice were examined at each time point of 1, 3, 6, 9, and 12 months. Human tissue blocks from PSP, FTDP-17, and ALS/PDC cases were cut and stained as described above.

Tau Protein Solubility in the CNS of Tg Mice

To study the solubility of tau proteins in the mouse CNS, cerebral cortical and spinal cord tissues of 1-, 3-, 6-, and 9-month Tg and wt mice were extracted with RAB Hi-Salt to generate the RAB-soluble fractions as described above. The pellets were rehomogenized with 1 M sucrose/RAB (0.1 M MES, 1 mM EGTA, and 0.5 mM $MgSO_4$ [pH 7.0]) and centrifuged at 50,000 × g for 20 min at 4°C. The resulting pellets were extracted with 1 ml/g RIPA buffer (50 mM Tris, 150 mM NaCl, 1% NP40, 5 mM EDTA, 0.5% sodium deoxycholate, and 0.1% SDS [pH 8.0]) and centrifuged to generate RIPA-soluble samples, the RIPA-insoluble pellets were reextracted with 70% FA, and quantitative Western blots were used to determine tau level in each fraction.

Determination of the Phosphorylation State of Tau in Tg Mice

To assess the phosphorylation state of Tg tau, cortical tissues from 6-month-old line 7 Tg mice were extracted as described above. A simplified protocol was adopted to generate the RAB-insoluble fractions. Briefly, the RAB-insoluble pellets were sonicated in sample buffer containing 0.2 g/ml sucrose, 18.5 mM Tris (pH 6.8), 2 mM EDTA, 80 mM DTT, and 2% SDS, and the 50,000 × g supernatants were used as insoluble Tg tau samples. Human PHF-tau, autopsy-derived adult tau, and fetal tau were prepared as described (Lee et al., 1991; Bramblett et al., 1992, 1993).

Determination of Tubulin and NF Protein Levels in Sciatic Nerves of Tg Mice

To determine the tubulin and NF protein levels in sciatic nerves, 10 mm segments of proximal sciatic nerve from line 7 Tg mice and age-matched wt mice (1, 3, 6, and 9 months) were harvested and individually homogenized in 500 μl of ice-cold RAB Hi-Salt buffer. After centrifugation at 50,000 × g for 40 min at 4°C, the supernatants were used for the analysis of tau and tubulin, whereas the pellets were used for NF analysis. Equal volumes (15 μl) of each sample were analyzed by quantitative Western blotting.

Electron Microscopy

Transmission EM was performed to study the ultrastructure of the inclusions. Tg mice and wt littermates at 6 and 12 months of age ($n = 4$) were deeply anesthetized and sacrificed by intracardiac perfusion with 10 ml of 0.1 M cacodylate buffer (pH 7.4) followed by 50 ml fixative (2% glutaraldehyde and 2% paraformaldehyde in 0.1 M cacodylate buffer). The L5 segments of the spinal cord and L5 ventral roots were removed and postfixed in 2% osmium tetroxide for 45 min at 4°C. The samples were embedded, sectioned, stained, and examined as described (Tu et al., 1995).

Postembedding immuno-EM was performed for Tg and wt mice (6 and 12 months, $n = 4$) by intracardiac perfusion with 10 ml of 0.1 M cacodylate buffer (pH 7.4) and 50 ml of fixative (0.2% glutaraldehyde, 2% paraformaldehyde, and 0.2% pricric in 0.1 M cacodylate buffer) followed by postfixation in fixative containing 0.2% glutaraldehyde, 4% paraformaldehyde, 0.2% pricric, and 0.1 M cacodylate overnight. The tissue blocks were quenched in 0.1 M Tris and 1 M glycine for 15 min, dehydrated with graded ethanol, and then infiltrated and embedded in LR-White resin (London Resin). Grids with ultrathin sections were blocked in PBS containing 5% donor horse serum and 0.2% cold water fish skin gelatin and incubated with

primary antibodies overnight at 4°C. Goat anti-mouse nanogold-IgG (for T14 and β-tubulin) or goat anti-rabbit nanogold-IgG (for NFL) (Nanoprobes) was used as secondary antibody.

Quantification of Axon Number, MT Density, and NF Density in Ventral Roots

The toluidine blue–stained semithin sections were used to count axon numbers in the L5 ventral roots of 6- and 12-month-old Tg and wt mice prepared for transmission EM (n = 3). To quantitate MTs and NFs, ten transversely sectioned axons from each ventral root were randomly chosen and photographed at 25,000× magnification by transmission EM. A template transparency containing identical hexagons with a defined area was overlaid on the micrographs, and the number of MTs and NFs in each hexagon was counted to generate MT and NT densities per unit area. The results were analyzed by Student's t test.

Fast Axonal Transport Studies

Twelve-month-old tau TG and age-matched mice (n = 3 per group) underwent laminectomy from segments T13 to L1 of the spinal cord under deep anesthesia. [^{35}S]methionine (300 μCi) in 0.8 μl of saline was microinjected into two sites of each side of the L5 ventral horn with a stereotaxic apparatus over a period of 5 min as previously described (Zhang et al., 1997). Animals were sacrificed 3 hr after microinjection, and the L5 ventral roots were removed, cut into five consecutive segments of 2 mm length (from proximal to distal), processed for SDS–PAGE, and subjected to quantitative Western blotting to assess fast axonal protein transport.

Antibodies

The following antibodies were used in this study: T14 (a mAb specific to human tau), 17026 (a rabbit polyclonal antibody made against the largest human recombinant tau), and Alz50 (a mAb specific for a conformation epitope found in PHFs), which are phosphorylation independent antibodies (Kosik et al., 1988; Trojanowski et al., 1989; Carmel et al., 1996); mAb T1 (Binder et al., 1985; Szendrei et al., 1993); mAb PHF1 (Greenberg and Davies, 1990; Lang et al., 1992; Otvos et al., 1994); mAb PHF6 (Hoffmann et al., 1997); mAb AT8 (Goedert et al., 1993, 1994); mAb AT270 (Goedert et al., 1994; Matsuo et al., 1994); mAb 12E8 (Seubert et al., 1995); and polyclonal rabbit antiserum T3P (Lee et al., 1991). Antibodies against NF subunits included mAb RMdO9 (nonphosphorylated NFH), mAb RMO55 (phosphorylated NFM), rat mAb TA51 (phosphorylated NFH and NFM), and polyclonal rabbit antiserum to NFL (Tu et al., 1995). In addition, a rat mAb to α-tubulin and a mouse mAb to β-tubulin were purchased, and a rat mAb (2.2B10) to GFAP (Tu et al., 1995) was also used.

Acknowledgments

We thank Dr. A. Hirano for providing tissue block of ALS/PDC; the Biomedical Imaging Core Facility of the University of Pennsylvania for assistance in the EM studies; Dr. M. L. Schmidt for PSP and FTDP-17 sections; and N. Shah, E. Heatherby, K. H. Szymczyk, and Grace Kim for technical assistance. This work was supported by grants from the National Institute on Aging.

Received May 4, 1999; revised September 8, 1999.

References

Andreadis, A., Brown, W.M., and Kosik, K.S. (1992). Structure and novel exons of the human tau gene. Biochemistry *31*, 10626–10633.

Binder, L.I., Frankfurter, A., and Rebhun, L.I. (1985). The distribution of tau in the mammalian central nervous system. J. Cell Biol. *101*, 1371–1378.

Borchelt, D.R., Davis, J., Fischer, M., Lee, M.K., Slunt, H.H., Ratovitsky, T., Regard, J., Copeland, N.G., Jenkins, N.A., Sisodia, S.S., and Price, D.L. (1996). A vector for expressing foreign genes in the brains and hearts of transgenic mice. Genet. Anal. *13*, 159–163.

Bramblett, G.T., Trojanowski, J.Q., and Lee, V.M.-Y. (1992). Regions with abundant neurofibrillary pathology in human brain exhibit a selective reduction in levels of binding-competent tau and accumulation of abnormal tau-isoforms (A68 proteins). Lab. Invest. *66*, 212–222.

Bramblett, G.T., Goedert, M., Jakes, R., Merrick, S.E., Trojanowski, J.Q., and Lee, V.M.-Y. (1993). Abnormal tau phosphorylation at Ser396 in Alzheimer's disease recapitulates development and contributes to reduced microtubule binding. Neuron *10*, 1089–1099.

Brion, J.-P., Tremp, G., and Octave, J.-N. (1999). Transgenic expression of the shortest human tau affects its compartmentalization and its phosphorylation as in the pretangle stage of Alzheimer's disease. Am. J. Pathol. *154*, 255–270.

Carmel, G., Mager, E.M., Binder, L.I., and Kuret, J. (1996). The structural basis of monoclonal antibody Alz50's selectivity for Alzheimer's disease pathology. J. Biol. Chem. *271*, 32789–32795.

Clark, L.N., Poorkaj, P., Wszolek, Z.K., Geschwind, D.H., Nasreddine, Z.S., Miller, B., Payami, H., Awert, F., Markopoulou, K., D'Souza, I., et al. (1998). Pathogenic implications of mutations in the tau gene in pallido-ponto-nigral degeneration and related chromosome 17–linked neurodegenerative disorders. Proc. Natl. Acad. Sci. USA *95*, 13103–13109.

Drechsel, D.N., Hyman, A.A., Cobb, M.H., and Kirschner, M.W. (1992). Modulation of the dynamic instability of tubulin assembly by the microtubule-associated protein tau. Mol. Biol. Cell *3*, 1141–1154.

D'Souza, I., Poorkaj, P., Hong, M., Nochlin, D., Lee, V.M.-Y., Bird, T.D., and Schellenberg, G.D. (1999). Missense and silent tau gene mutations cause frontotemporal dementia with parkinsonism - chromosome 17 type, by affecting multiple alternative RNA splicing regulatory elements. Proc. Natl. Acad. Sci. USA *96*, 5598–5603.

Goedert, M., and Jakes, R. (1990). Expression of separate isoforms of human tau protein: correlation with the tau pattern in brain and effects on tubulin polymerization. EMBO J. *9*, 4225–4230.

Goedert, M., Spillantini, M.G., Jakes, R., Rutherford, D., and Crowther, R.A. (1989). Multiple isoforms of human microtubule–associated protein tau: sequences and localization in neurofibrillary tangles of Alzheimer's disease. Neuron *3*, 519–526.

Goedert, M., Jakes, R., Crowther, R.A., Six, J., Lubke, U., Vandermeeren, M., Cras, P., Trojanowski, J.Q., and Lee, V.M.-Y. (1993). The abnormal phosphorylation of tau protein at Ser-202 in Alzheimer disease recapitulates phosphorylation during development. Proc. Natl. Acad. Sci. USA *90*, 5066–5070.

Goedert, M., Jakes, R., Crowther, R.A., Cohen, P., Vanmechelen, E., Vandermeeren, M., and Cras, P. (1994). Epitope mapping of monoclonal antibodies to the paired helical filaments of Alzheimer's disease: identification of phosphorylation sites in tau protein. Biochem. J. *301*, 871–877.

Goedert, M., Trojanowski, J.Q., and Lee, V.M.-Y. (1997). The neurofibrillary pathology of Alzheimer's disease. In The Molecular and Genetic Basis of Neurological Diseases. S.B. Prusiner et al., eds. (Boston: Butterworth-Heinemann Press), pp. 613–627.

Goetz, J., Probst, A., Spillantini, M.G., Schafer, T., Jakes, R., Buerki, K., and Goedert, M. (1995). Somatodendritic localization and hyperphosphorylation of tau protein in transgenic mice expressing the longest human brain tau isoform. EMBO J. *14*, 1304–1313.

Greenberg, S.G., and Davies, P. (1990). A preparation of Alzheimer paired helical filaments that displays distinct tau proteins by polyacrylamide gel electrophoresis. Proc. Natl. Acad. Sci. USA *87*, 5827–5831.

Hirano, A., Malamud, N., and Kurland, L.T. (1961). Parkinsonism dementia complex: an endemic disease on the island of Guam - pathological features. Brain *84*, 642–661.

Hoffmann, R., Lee, V.M.-Y., Leight, S., Varga, I., and Otvos, L., Jr. (1997). Unique Alzheimer's disease paired helical filament specific epitopes involve double phosphorylation at specific sites. Biochemistry *36*, 8114–8124.

Hong, M., Zhukareva, V., Vogelsberg-Ragaglia, V., Wszolek, Z., Reed, L., Miller, B.I., Geschwind, D.H., Bird, T.D., McKeel, D., Goate, A., et al. (1998). Mutation-specific functional impairments in distinct tau isoforms of hereditary FTDP-17. Science *282*, 1914–1917.

Hutton, M., Lendon, C.L., Rizzu, P., Baker, M., Froelich, S., Houlden, H., Pickering-Brown, S., Chakraverty, S., Isaacs, A., Grover, A., et

al. (1998). Association of missense and 5′-splice-site mutations in tau with the inherited dementia FTDP-17. Nature *393*, 702–705.

Iijima, M., Tabira, T., Poorkaj, P., Schellenberg, G.D., Trojanowski, J.Q., Lee, V.M.-Y., Schmidt, M.L., Takahashi, K., Nabika, T., Matsumoto, T., et al. (1999). A distinct familial presenile dementia with a novel missense mutation in the tau gene. Neuroreport *10*, 497–501.

Kato, T., Hirano, A., Weinberg, M.N., and Jacobs, A.K. (1986). Spinal cord lesions in progressive supranuclear palsy: some new observations. Acta Neuropathologica *71*, 11–14.

Kosik, K.S., Orecchio, L.D., Binder, L., Trojanowski, J.Q., Lee, V.M.-Y., and Lee, G. (1988). Epitopes that span the tau molecule are shared with paired helical filaments. Neuron *1*, 817–825.

Lang, E., Szendrei, G.I., Lee, V.M.-Y., and Otvos, L., Jr. (1992). Immunological and conformation characterization of a phosphorylated immunodominant epitope on the paired helical filaments found in Alzheimer's disease. Biochem. Biophys. Res. Commun. *187*, 783–790.

Lee, V.M.-Y., Balin, B.J., Otvos, L., Jr., and Trojanowski, J.Q. (1991). A68: a major subunit of paired helical filaments and derivatized forms of normal Tau. Science *251*, 675–678.

Matsumoto, S., Hirano, A., and Goto, S. (1990). Spinal cord neurofibrillary tangles of Guamanian amyotrophic lateral sclerosis and parkinsonism–dementia complex: an immunohistochemical study. Neurology *40*, 975–979.

Matsuo, E.S., Shin, R.W., Billingsley, M.L., Van deVoorde, A., O'Connor, M., Trojanowski, J.Q., and Lee, V.M.-Y. (1994). Biopsy-derived adult human brain tau is phosphorylated at many of the same sites as Alzheimer's disease paired helical filament tau. Neuron *13*, 989–1002.

Nakazato, Y., Sasaki, A., Hirato, J., and Ishida, Y. (1984). Immunohistochemical localization of neurofilament protein in neuronal degenerations. Acta Neuropathologica *64*, 30–36.

Otvos, L., Jr., Feiner, L., Lang, E., Szendrei, G.I., Goedert, M., and Lee, V.M.-Y. (1994). Monoclonal antibody PHF-1 recognizes tau protein phosphorylated at serine residues 396 and 404. J. Neurosci. Res. *39*, 669–673.

Perry, G., Rizzuto, N., Autilio-Gambetti, L., and Gambetti, P. (1985). Paired helical filaments from Alzhemier's disease patients contain cytoskeletal components. Proc. Natl. Acad. Sci. USA *82*, 3916–3920.

Poorkaj, P., Bird, T.D., Wijsman, E., Nemens, E., Garruto, R.M., Anderson, L., Andreadis, A., Wiederholt, W.C., Raskind, M., and Schellenberg, G.D. (1998). Tau is a candidate gene for chromosome 17 frontotemporal dementia. Ann. Neurol. *43*, 815–825.

Reed, L.A., Schmidt, M.L., Wszolek, Z.K., Balin, B.J., Soontornniyomkij, V., Lee, V.M.-Y., Trojanowski, J.Q., and Schelper, R.L. (1998). The neuropathology of a chromosome 17–linked autosomal dominant parkinsonism and dementia ("pallido-ponto-nigral degeneration"). J. Neuropathol. Exp. Neurol. *57*, 588–601.

Rizzu, P., Van Swieten, J.C., Joosse, M., Hasegawa, M., Stevens, M., Tibben, A., Niermeijer, M.F., Hillebrand, M., Ravid, R., Oostra, B.A., et. al. (1999). High prevalence of mutations in the microtubule-associated protein tau in a popolation study of frontotemporal dementia in the Netherlands. Am. J. Hum. Genet. *64*, 414–421.

Schmidt, M.L., Lee, V.M.-Y., and Trojanowski, J.Q. (1990). Relative abundance of tau and neurofilament epitopes in hippocampal neurofibrillary tangles. Am. J. Pathol. *136*, 1069–1075.

Schmidt, M.L., Lee, V.M.-Y., and Trojanowski, J.Q. (1991). Comparative epitope analysis of neuronal cytoskeletal proteins in Alzheimer's disease senile plaque neurites and neuropil threads. Lab. Invest. *64*, 352–357.

Seubert, P., Mawal-Dewan, M., Barbour, R., Jakes, R., Goedert, M., Johnson, G.V., Litersky, J.M., Schenk, D., Lieberburg, I., Trojanowski, J.Q., and Lee, V.M.-Y. (1995). Detection of phosphorylated Ser262 in fetal tau, adult tau, and paired helical filament tau. J. Biol. Chem. *270*, 18917–18922.

Shankar, S.K., Yanagihara, R., Garruto, R.M., Grundke-Iqbal, I., Kosik, K.S., and Gajdusek, D.C. (1989). Immunocytochemical characterization of neurofibrillary tangles in amyotrophic lateral sclerosis and parkinsonism–dementia of Guam. Ann. Neurol. *25*, 146–151.

Spillantini, M.G., Bird, T.D., and Ghetti, B. (1998a). Frontotemporal dementia and Parkinsonism linked to chromosome 17: a new group of tauopathies. Brain Pathol. *8*, 387–402.

Spillantini, M.G., Murrell, J.R., Goedert, M., Farlow, M.R., Klug, A., and Ghetti, B. (1998b). Mutation in the tau gene in familial multiple system tauopathy with presenile dementia. Proc. Natl. Acad. Sci. USA *95*, 7737–7741.

Szendrei, G.I., Lee, V.M.-Y., and Otvos, L., Jr. (1993). Recognition of the minimal epitope of monoclonal antibody Tau-1 depends upon the presence of a phosphate group but not its location. J. Neurosci. Res. *34*, 243–249.

Tomonaga, M. (1977). Ultrastructure of neurofibrillary tangles in progressive supranuclear palsy. Acta Neuropathologica *37*, 177–181.

Trojanowski, J.Q., Schuck, T., Schmidt, M.L., and Lee, V.M.-Y. (1989). Distribution of tau proteins in the normal human central and peripheral nervous system. J. Histochem. Cytochem. *37*, 209–215.

Tu, P.H., Elder, G., Lazzarini, R.A., Nelson, D., Trojanowski, J.Q., and Lee, V.M.-Y. (1995). Over-expression of the human NFM subunit in transgenic mice modifies the level of endogenous NFL and the phosphorylation state of NFH subunits. J. Cell Biol. *129*, 1629–1640.

Tu, P.H., Gurney, M.E., Julien, J.-P., Lee, V.M.-Y., and Trojanowski, J.Q. (1997). Oxidative stress, mutant SOD1, and neurofilament pathology in transgenic mouse models of human motor neuron disease. Lab. Invest. *76*, 441–456.

Weingarten, M.D., Lockwood, A.H., Hwo, S.Y., and Kirschner, M.W. (1975). A protein factor essential for microtubule assembly. Proc. Natl. Acad. Sci. USA *72*, 1858–1862.

Yoshida, H., and Ihara, Y. (1993). Tau in paired helical filaments is functionally distinct from fetal tau: assembly incompetence of paired helical filament–tau. J. Neurochem. *61*, 1183–1186.

Zhang, B., Tu, P.-H., Abtahian, F., Trojanowski, J.Q., and Lee, V.M.-Y. (1997). Neurofilaments and orthograde transport are reduced in ventral root axons of transgenic mice that express human SOD1 with a G93A mutation. J. Cell Biol. *139*, 1307–1315.